Acta Crystallographica Section D
Biological Crystallography
ISSN 0907-4449

Crystallization and preliminary X-ray analysis of pseudo-merohedrally twinned crystals of the full-length β_2 subunit of the Kv1 K^+ channel from *Rattus norvegicus*

Tatsuro Shimamura,[a] Oleg Shamotienko,[b] Sobia Akhtar,[b] J. Oliver Dolly[b] and So Iwata[a]*

[a]Division of Biomedical Sciences, Imperial College, London SW7 2AZ, England, and [b]Department of Biological Sciences, Imperial College, London SW7 2AZ, England

Correspondence e-mail: s.iwata@ic.ac.uk

Received 15 December 2003
Accepted 25 February 2004

The eukaryotic Kv1 voltage-gated K^+ channel is composed of four α subunits and four β subunits. The full-length β_2 subunit from *Rattus norvegicus* has been expressed in *Escherichia coli*, purified and then crystallized. A careful molecular-replacement study using the structure of the truncated β_2 subunit reveals that the crystals are perfectly pseudo-merohedrally twinned. While the apparent space group of the crystals was $P42_12$, the real space group was shown to be $P2_12_12$, with unit-cell parameters a = 222.6, b = 222.6, c = 82.3 Å. An asymmetric unit of the crystal contains two β_2 tetramers (MW = 340 kDa). A data set was collected from a crystal to 2.0 Å resolution, with 266 659 independent observations (93.0% complete) and $R_{\rm merge}$ = 0.06. Although the crystals are perfectly twinned, they are still suitable for structural determination by molecular replacement using the truncated β_2-subunit structure.

1. Introduction

Voltage-gated K^+ channels are involved in a variety of functions including control of neural excitability, shaping of the action potentials, determining the inter-spike interval and indirectly regulating transmitter release (Jan & Jan, 1997). They control the electric potential across cell membranes by mediating the rapid selective diffusion of K^+ down their electrochemical gradient. The Kv1 family of eukaryotic voltage-gated K^+ channels are composed of four α subunits and four β subunits (Parcej *et al.*, 1992; Orlova *et al.*, 2003). Four α subunits form the transmembrane channel for K^+ conduction and voltage-dependent gating. Four soluble β subunits are attached to the cytoplasmic face of the α tetramer. The detailed roles of the β subunits remain unknown, although β_1 accelerates inactivation of the channel (Rettig *et al.*, 1994). The β subunits have a conserved core related in amino-acid sequence to aldo–keto reductases, although the specific substrate has not been detected. Moreover, the β subunits have a mobile N-terminal extension that has been revealed to be involved in the inactivation of the channel (Zhou *et al.*, 2001). The extent of inactivation differs depending on the subtype of the β-subunit family. The inactivation of the K^+ channel shapes the electrical signalling properties of many types of nerve, muscle and other cells. Of the β-subunit family, only the structure of the β_2 subunit, a subtype of the β subunit, has been solved so far; however, the β_2 subunit was expressed as a truncated form without the crucial N-terminal extension in order to prevent protein aggregation and facilitate crystallization (Gulbis *et al.*, 1999, 2000). In order to understand the inactivation mechanism of the K^+ channel controlled by the β subunit, the X-ray structure of the full-length β subunit is indispensable.

Here, we report the crystallization of the full-length β_2 subunit from *Rattus norvegicus*, which diffracted to 2.0 Å resolution.

2. Materials and methods

2.1. Expression

The gene coding for the full-length β_2 subunit from *R. norvegicus* was cloned into the pET20b vector (Novagen, Germany) and overexpressed under control of the T7 promoter in *Escherichia coli*. *E. coli* BL21 (DE3) harbouring the expression plasmid was cultivated in LB medium containing 50 μg ml^{-1} ampicillin and 34 μg ml^{-1} chloramphenicol at 310 K. When the OD_{600} reached 0.6, expression of the full-length β_2 subunit was induced with 0.8 m*M* IPTG for 4 h at 310 K. The cells were harvested by centrifugation and stored at 193 K.

2.2. Purification

The cell pellet was thawed and resuspended in 20 m*M* HEPES pH 7.5, 0.5 *M* NaCl, 5 m*M* KCl, 5 m*M* imidazole (buffer *A*) and the resultant slurry sonicated. After removal of the cell debris by centrifugation, the supernatant was applied onto an Ni–NTA superflow column (Qiagen, Germany) equilibrated with buffer *A*. The column was subsequently washed with five column volumes of buffer *B* (20 m*M* HEPES pH 7.5, 0.5 *M* NaCl, 5 m*M* KCl, 50 m*M* imidazole) before the bound

protein was eluted with a linear gradient of 0–100% buffer *C* (20 m*M* HEPES pH 7.5, 0.5 *M* NaCl, 5 m*M* KCl, 500 m*M* imidazole). The purity of the protein was assessed by SDS–PAGE. Fractions containing the β_2 subunit were pooled and concentrated using a 10 kDa cutoff filter (Vivaspin, Germany). The protein was finally concentrated to 10 mg ml^{-1} and then used for crystallization trials.

2.3. Initial crystallization

Crystals were grown by the hanging-drop vapour-diffusion method. The protein sample was mixed with reservoir solution in a 1:1 ratio and left to equilibrate at 277 K. Initial crystals were obtained using several conditions from Crystal Screen 1 and 2 (Hampton Research, USA) containing polyethylene glycol 400 (PEG 400), jeffamine M-600 or 2-propanol as precipitants. Among these conditions, No. 12 [0.1 *M* HEPES pH 7.5, 0.2 *M* $MgCl_2$, 30%(*v*/*v*) 2-propanol] and No. 27 [0.1 *M* HEPES pH 7.5, 0.2 *M* trisodium citrate, 20%(*v*/*v*) 2-propanol] from Crystal Screen 1 produced good-looking crystals. Using these conditions, crystals appeared after a few days and stopped growing within two weeks.

2.4. Optimization of crystallization conditions

Crystals obtained from conditions Nos. 12 and 27 of Crystal Screen 1 diffracted to 3.5 Å. The low-resolution limit could be a consequence of the unsuitable freezing conditions caused by the evaporation of 2-propanol during crystal handling. Screening of the non-volatile organic alcohol used as a precipitant and optimization of the concentration improved the freezing conditions and the subsequent diffraction quality of the crystals. The final optimized crystallization condition after iterative optimization cycles was 0.1 *M* HEPES pH 7.5, 55% 2-methyl-2,4-pentanediol (MPD), 5 m*M* NaCl. Crystals appeared after one week and reached maximum dimensions of 0.05 × 0.05 × 0.2 mm within two weeks.

Figure 1
Crystal of the full-length β_2 subunit of the voltage-gated K^+ channel from *R. norvegicus*. The crystal has approximate dimensions of 0.05 × 0.05 × 0.2 mm.

2.5. Data collection and crystallographic analysis

Crystals were mounted in nylon loops (Hampton Research) and frozen in liquid nitrogen. Data collection from frozen crystals was performed at 100 K. Diffraction data to 2.0 Å were collected on beamline ID29 of the European Synchrotron Radiation Facility (ESRF) using an ADSC Quantum 4 CCD detector. A wavelength of 0.9773 Å and a crystal-to-detector distance of 240 mm were used. The beam size, oscillation range and exposure time were 100 × 100 µm, 0.3°and 15 s per frame, respectively. Data integration was performed with *DENZO* and scaling was performed with *SCALEPACK*; both programs are from the *HKL* program package (Otwinowski & Minor, 1997). All data better than $-3.0\sigma(I)$ were used for scaling. Data statistics are given in Table 1. A self-rotation function was calculated with the program *POLARRFN* (Kabasch, unpublished work; Collaborative Computational Project, Number 4, 1994) using a radius of integration of 29 Å and data in the resolution range 5–12 Å. Molecular-replacement trials were performed with the program *AMoRe* (Navaza, 2001) using the N-terminal truncated β_2 subunit structure (PDB entry 1exb; Gulbis *et al.*, 2000) as a search model.

3. Results and discussion

Whereas the N-terminally truncated β_2 subunit used for the previous structure determination was expressed in Sf9 cells (Gulbis *et al.*, 1999, 2000), large amounts of the full-length rat β_2 subunit were expressed in *E. coli* cells using the pET20b vector. The expressed recombinant β_2 subunit was confirmed to exist in the soluble fraction by SDS–PAGE of the supernatant after sonication of the cells and removal of the debris. After optimization of the concentration of MPD and the type of salt, small but well diffracting crystals were obtained from the condition mentioned above (Fig. 1). The crystals diffracted to 2.0 Å, which is better than that found with the crystals of the N-terminally truncated β_2 subunit (Gulbis *et al.*, 2000).

It was possible to collect a complete data set from one of the largest crystals. The crystals apparently belong to the tetragonal space group $P42_12$, with unit-cell parameters $a = b = 222.6$, $c = 82.3$ Å. Assuming the crystallographic asymmetric unit to contain a tetramer, the Matthews coefficient (V_M; Matthews, 1968) and solvent content of the crystals are 3.0 Å^3 Da^{-1} and 59.4%, respectively.

Table 1
Data statistics.

Statistics for the last shell (2.1–2.0 Å) are given in parentheses.

Space group	$P2_12_12$
Resolution (Å)	2.0
Unit-cell parameters (Å)	a = 222.6, b = 222.6, c = 82.3
Total observations	614510
Unique observations	266659
Completeness (%)	93.0 (80.0)
R_{merge} (%)	6.0 (38.2)
Average $I/\sigma(I)$	15.1 (2.3)

Molecular replacement was performed using the structure of the truncated β_2-monomer structure (PDB entry 1exb: Gulbis *et al.*, 2000), which contained 90% of the amino-acid residues of the full-length β_2 subunit; however, it was not possible to find a clear solution. In order to solve this problem, we took advantage of the molecular fourfold axis of the β_2-subunit tetramer. The structure factors were extended to cover the *P*1 cell and the molecular-replacement search was repeated using the tetramer as a model. This yielded a clear solution with eight tetramers in the unit cell. In the solution, two tetramers form a face-to-face octamer with 422 point symmetry. A similar arrangement is observed in the truncated β_2-subunit crystals (Gulbis *et al.*, 1999). The packing clearly showed the real space group of the crystals

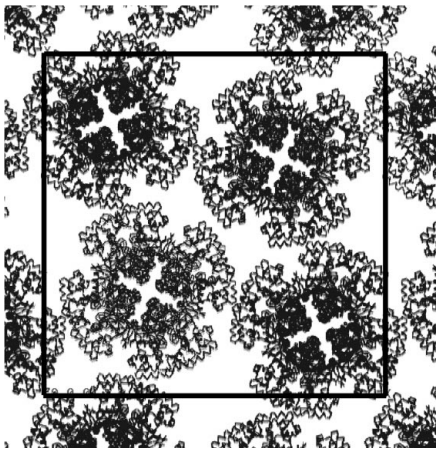

Figure 2
Crystal packing of the molecular-replacement solution. The box indicates the unit cell of the crystal.

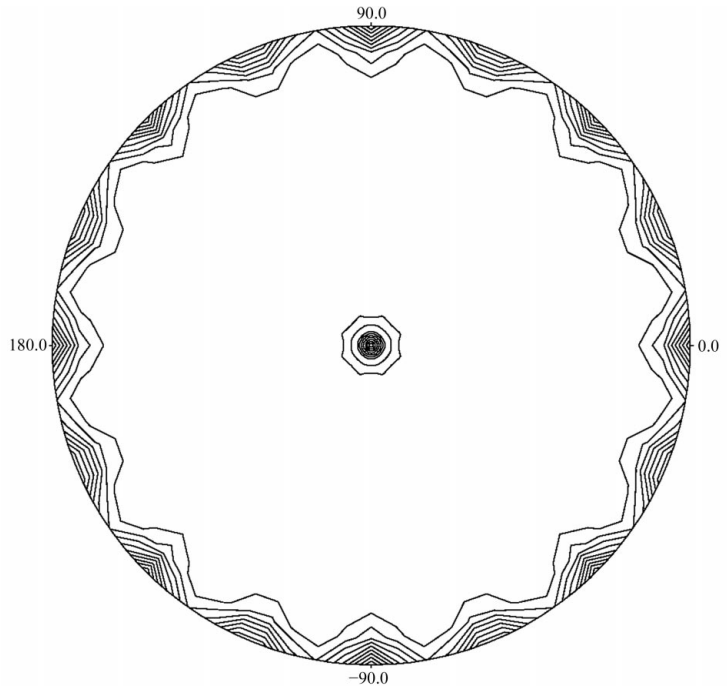

Figure 3
Self-rotation function map of a crystal calculated in the resolution range 12–5 Å and plotted for $\kappa = 180^\circ$ section.

to be $P2_12_12$, with unit-cell parameters $a = 222.6$, $b = 222.6$, $c = 82.3$ Å. The molecular-replacement search using the data extended to $P2_12_12$ gave a unique solution with a correlation factor of 68.0% and an R factor of 39.9% (Fig. 2). The crystallographic asymmetric unit contains one octamer of the β_2 subunit. The apparent space group $P42_12$ was initially assigned owing to the perfect hemihedral twinning with twinning operator $(-k, h, l)$. This is possible because the a and b axes of the original orthorhombic cell are the same length. Perfect twinning is also supported by the fact that the $R_{\rm merge}$ for the data set scaled as $P42_12$ (6.6%) is only slightly higher than that for $P2_12_12$ (6.0%).

The self-rotation function analysis of the data supports the obtained molecular-replacement solution (Fig. 3). In the $\kappa = 180^\circ$ section, in addition to the crystallographic twofold axes ($\omega = 0$, $\varphi = 0^\circ$ and $\omega = 90$, $\varphi = 0$, 90, 180, 270°), the apparent twofold axes derived from the twinning operator are clearly observed ($\omega = 90$, $\varphi = 45$, 135, 225, 315°). The rest of the peaks on the $\omega = 90^\circ$ circle are from non-crystallographic twofold axes derived from the observed octamer with 422 point symmetry.

Because a structure for the truncated β_2 subunit is available and the resolution of the data for the full-length β_2 subunit is reasonably high, it is possible to refine the structure in spite of the twinning problems using programs such as *CNS* (Brünger *et al.*, 1998) or *SHELX*97 (Sheldrick & Schneider, 1997). Structure refinement is in progress.

References

Brünger, A. T., Adams, P. D., Clore, G. M., DeLano, W. L., Gros, P., Grosse-Kunstleve, R. W., Jiang, J.-S., Kuszewski, J., Nilges, M., Pannu, N. S., Read, R. J., Rice, L. M., Simonson, T. & Warren, G. L. (1998). *Acta Cryst.* D**54**, 905–921.
Collaborative Computational Project, Number 4 (1994). *Acta Cryst.* D**50**, 760–763.
Gulbis, J. M., Mann, S. & MacKinnon, R. (1999). *Cell*, **97**, 943–952.
Gulbis, J. M., Zhou, M., Mann, S. & MacKinnon, R. (2000). *Science*, **289**, 123–127.
Jan, L. Y. & Jan, Y. N. (1997). *Annu. Rev. Neurosci.* **20**, 91–123.
Matthews, B. W. (1968). *J. Mol. Biol.* **33**, 491–497.
Navaza, J. (2001). *Acta Cryst.* D**57**, 1367–1372.
Orlova, E. V., Papakosta, M., Booy, F. P., van Heel, M. & Dolly, J. O. (2003). *J. Mol. Biol.* **326**, 1005–1012.
Otwinowski, Z. & Minor, W. (1997). *Methods Enzymol.* **276**, 307–326.
Parcej, D. N., Scott, V. E. & Dolly, J. O. (1992). *Biochemistry*, **31**, 11084–11088.
Rettig, J., Heinemann, S. H., Wunder, F., Lorra, C., Parcej, D. N., Dolly, J. O. & Pongs, O. (1994). *Nature (London)*, **369**, 289–294.
Sheldrick, G. M. & Schneider, T. R. (1997). *Methods Enzymol.* **277**, 319–343.
Zhou, M., Morais-Cabral, J. H., Mann, S. & MacKinnon, R. (2001). *Nature (London)*, **411**, 657–661.